CHAPTER 37

DEVELOPMENT OF A THIRD GENERATION SHALLOW-WATER WAVE MODEL WITH UNSTRUCTURED SPATIAL MESHING

Michel BENOIT [1], Frédéric MARCOS[1], Françoise BECQ [2]

Abstract
A numerical third-generation wave model dedicated both to deep water and near-shore applications is presented and applied to several test-cases to highlight its capabilities. Among its main features, this model uses a finite-elements technique for the discretization of the modelled area, which makes it suitable to represent complex bottom topographies and irregular shorelines. Furthermore, the piece-wise ray method used for wave propagation allows to use rather large time-steps, which in turn allows to keep the computational time at a very moderate level. The implementation of shallow-water physics in the model is also described, in particular with respect to depth-induced breaking. Several applications of the model are presented and compared to field or laboratory data for their validation. Finally, the main research and development items are mentioned and discussed.

1. INTRODUCTION

Although originally developed for deep water applications and meteorological purpose (e.g. WAMDI Group, 1988), spectral "phase-averaged" wave models are presently being extended towards the near-shore and coastal domains. This extension implies first to improve the physics of the numerical models so that they become able to reproduce shallow-water effects. Several efforts have already been attempted in this way by developing numerical formulations for bottom friction, depth-induced breaking and non-linear interactions between triplets of waves (the so-called "triad-interactions") (e.g. Ris et al., 1994 ; Van Vledder et al., 1994).

A second point to consider is the ability of the model to deal with the complex bottom topography of coastal and near-shore areas. Compared to oceanic applications, these shallow-water domains usually need a finer spatial discretization to properly represent bathymetric gradients and irregular shorelines. This requires a number of properties from the numerics of the wave model (discretization techniques, integration schemes) which are usually not encountered in present third-generation wave models. For instance, if one wishes to apply the WAM model to local areas, the size of the finite-difference spatial grid has to be decreased over the whole domain, which highly increases the number of computational points and

---

[1]   Research Engineer — Maritime Group
[2]   PhD Student — Maritime Group
     EDF - Laboratoire National d'Hydraulique,   6, quai Watier   78400 CHATOU,   FRANCE

often leads to use nested grids. Furthermore, the explicit scheme for wave propagation in WAM will then imply a strong decrease of the time-step in order to ensure that the Courant Number remains lower than 1. This, in turn, will cause a significant increase of the computational time, so that the computation will likely become unrealistic at an operational stage.

This paper deals with the development of a third generation spectral wave code applicable to deep water oceans, but also dedicated to shallow-water domains. This model, named TOMAWAC (which stands for "TELEMAC-based Operational Model Addressing Wave Action Computation"), is included in the TELEMAC modelling package developed by LNH, which contains numerous finite elements modules covering a wide range of maritime hydrodynamics applications.

The TOMAWAC model is presented in Section 2. Speeial attention to the implementation and validation of depth-induced breaking is paid in Section 3. Section 4 presents the application of the model on a test-case of waves propagating on a current whirl. In Section 5, the model is applied to the simulation of an actual storm in the North-eastern part of the Atlantic Ocean and in the Channel. Finally, present and future research items are presented and discussed in Section 6.

2. PRESENTATION OF TOMAWAC WAVE MODEL

2.1 Main modelling equations of TOMAWAC

TOMAWAC solves the wave action conservation equation (or wave action balance equation) in spherical or Cartesian co-ordinates for infinite or finite water depth. The wave action density N is defined as the ratio of directional variance density F to relative (or intrinsic) angular frequency σ : $N = F / \sigma$.

The directional variance density $F(f, \theta)$ corresponds to the "classical" directional spectrum of waves and models the way the wave energy (or variance) spreads over frequency f and direction θ.

In the presence of a current field $\vec{U}$, the action density is conserved (Bretherton and Garret, 1968). This leads to the following equation for the variance density $\tilde{F}(x, y, f_r, \theta, t)$, expressed in TOMAWAC as a function of time t, spatial Cartesian co-ordinates x and y, direction of propagation θ and relative frequeney f_r :

$$\frac{\partial(B.\tilde{F})}{\partial t} + C_x \frac{\partial(B.\tilde{F})}{\partial x} + C_y \frac{\partial(B.\tilde{F})}{\partial y} + C_\theta \frac{\partial(B.\tilde{F})}{\partial \theta} + C_{fr} \frac{\partial(B.\tilde{F})}{\partial fr} = B.Q \tag{1}$$

with : $F(f,\theta) = \dfrac{C_g}{C_g + \vec{U}.\vec{k}/k} \tilde{F}(f_r,\theta)$

The absolute angular frequency $\omega = 2\pi.f$ (as observed in a fixed frame of reference) is related to the relative angular frequency $\sigma = 2\pi.f_r$ (as observed in a frame moving with the speed $\vec{U}$) by the Doppler equation : $\omega = \sigma + \vec{k}.\vec{U}$.
where k is the wave-number vector, as given by the dispersion relation for linear waves as a function of water depth d : $\sigma^2 = g k \tanh(k.d)$

The transfer rates in space, direction and relative frequency are computed according to the linear wave theory :

$$C_x = Cg.\sin \theta + U_x \qquad C_\theta = -\frac{1}{k}\frac{\partial \sigma}{\partial d}\frac{\partial d}{\partial \vec{n}} - \frac{\vec{k}}{k}.\frac{\partial \vec{U}}{\partial \vec{n}}$$

$$C_y = Cg.\cos \theta + U_y \qquad C_{fr} = \frac{1}{2\pi}\left(\frac{\partial \sigma}{\partial d}\left(\frac{\partial d}{\partial t} + \vec{U}.\overrightarrow{\text{grad}}\, d\right) - C_g \vec{k}.\frac{\partial \vec{U}}{\partial \vec{s}}\right)$$

$\vec{n}$ is the direction perpendicular to wave propagation direction and $\vec{s}$ corresponds to the direction of propagation (given by θ). The coefficient B results from the fact that the conservation equation must be basically written for the action density expressed as a function of wave number : $B = C.C_g / (2\pi \sigma^2)$.

$C = \sigma / k$ and $C_g = \partial\sigma / \partial k$ are the phase and group speeds respectively.

The TOMAWAC model is unsteady (variable wind forcing conditions usually given by the wind-speed 10 m above the sea surface), but the current field $\vec{U}$ is assumed to be steady in version 1.2 of the code, as well as the water depth.

2.2 Modelisation of source and sink terms in TOMAWAC

In the Q term at the right-hand side of the balance equation (1), TOMAWAC 1.2 operationally includes the following physical processes : generation by wind (Q_{in}), dissipation by white-capping (Q_{wc}), bottom friction (Q_{bf}) and depth-induced breaking (Q_{br}), non-linear interactions between quadruplets of frequencies (Q_{nl4}). For each of these processes, several state-of-the-art formulations, calibrated against data from experimental campaigns in the field, are available in TOMAWAC and summarized in Table 1. The presentation of all the formulations is clearly out of the scope of this paper and can be found in the mentioned references. However, a more detailed presentation of depth-induced breaking is given in Section 3. In addition to these processes, a term modelling the non-linear transfers between triads of waves in shallow water (Eldeberky and Battjes, 1995) is presently under development and will be soon operational for use.

	Formulation 1	Formulation 2	Formulation 3
Q_{in} wind input	Janssen (1991)	Snyder et al. (1981) + u* from drag law	Snyder et al. (1981) + u* from Charnock
Q_{wc} white-capping	Komen et al. (1984)	Janssen (1991)	
Q_{nl4} quadruplets	Hasselmann et al. (1985)	Webb (1978) (under development)	
Q_{bf} bot. friction	Bouws and Komen (1983) + JONSWAP	Madsen et al. (1988)	Christoffersen and Jonsson (1985)
Q_{br} surf-breaking	Battjes and Janssen (1978)	Thornton and Guza (1983)	Roelvink (1993)

Table 1 : **Review of source and sink terms available in TOMAWAC 1.2.**

2.3 Numerical aspects of TOMAWAC

2.3.1 Spatial and spectral discretizations

Finite elements spatial discretization

Spectral wave models usually use finite differences grids for spatial meshing. This may however become a limitation for nearshore applications, where complex bathymetry and irregular shoreline often require a refined resolution. As already mentioned in the introduction, the first solution to this problem is to use nested grids, but this implies an heavy management of input/output files, complicates programming and significantly increases the computational effort.

The finite elements technique used in TOMAWAC (and in all the models of the TELEMAC system as well) overcomes this problem quite elegantly because the user can determine locally the size of the mesh and then optimize the number of nodes according to the accuracy expected in the various parts of the computational domain. The maritime area to be modelled is then discretized in a number of triangular elements whose size may be varied according to the desired resolution. This unique feature allows for instance to have on a same grid large oceanic areas (with mesh size in the order of several hundreds of kilometres) and nearshore areas (with mesh size in the order of one kilometre or less). Examples of spatial grids used by TOMAWAC are given in the following sections of this paper dealing with applications and validation test-cases.

Directional-spectral discretization

The range $[0 ; 2\pi]$ of wave directions is discretized in a number of equally spaced directions. This number of directions usually lies between 12 ($\Delta\theta = 30°$) and 72 ($\Delta\theta = 5°$). The discretized frequencies follow a logarithmic distribution ($f_{i+1} = (1+\epsilon).f_i$). The number of frequencies usually lies between 15 and 30. This results in a directional-spectral grid for the directional wave spectrum which is regular over directions and logarithmic over frequencies.

2.3.2 Numerical schemes

The wave action balance equation is solved in TOMAWAC by a fractional step method, including :

• a convection step (left-hand side of the balance equation (1)) :

$$\frac{\partial(B.\widetilde{F})}{\partial t} + \vec{V}.\overrightarrow{\text{grad}}(B.\widetilde{F}) = 0 \quad \text{with :} \quad \vec{V} = (C_x; C_y; C_\theta; C_{fr})$$

• and a source terms integration step (right-hand side of the equation (1)) :

$$\frac{\partial(B.\widetilde{F})}{\partial t} = B.Q \quad \text{which reduces to :} \quad \frac{\partial\widetilde{F}}{\partial t} = Q \quad \text{as B is independent of time.}$$

Propagation step :

The convection step is treated by a piece-wise ray method or method of characteristics. Due to the fact that the convector field is stationary, the characteristics curve have to be computed only once, at the beginning of computation. The results are stored in computer memory. At each time step, the convection step is thus reduced to an interpolation, which allows to save a good amount of computing time.

Source terms step

The source terms integration is carried out through a weighted implicit scheme :

$$\frac{\widetilde{F}^{n+1} - \widetilde{F}^*}{\Delta t_s} = \alpha.Q^* + (1-\alpha).Q^{n+1}$$

where $\widetilde{F}^*$ is the value of the variance spectrum after the propagation step and Q^* represent the value of source-terms based on $\widetilde{F}^*$.

Choosing $\alpha = 0$ ($\alpha = 1$) makes the scheme fully implicit (explicit). In one selects $\alpha = 0.5$, this scheme reduces to the semi-implicit scheme used in the WAM model (WAMDI Group, 1988).

2.3.3 Vectorization

TOMAWAC is fully vectorized and may be run either on super-computers or on workstations, depending on the size of the computational domain.

3. IMPLEMENTATION OF DEPTH-INDUCED BREAKING IN TOMAWAC

The modelling in TOMAWAC of energy dissipation due to depth-induced breaking is achieved by solving two successive problems : (i) estimation of the total energy dissipation due to breaking for the whole directional wave spectrum and (ii) distribution of this total dissipation over both frequencies and directions.

(i) Total dissipation of wave energy due to breaking:

The transformation of statistical parameters of an incident random wave train across the surf zone can be basically treated by two classes of models both based on the wave energy balance. The "probabilistic models" are based on a wave-by-wave approach (e.g. Dally, 1992) and offer a detailed description of the transformation of wave height distribution. This type of models was however not selected in TOMAWAC because of their important computational cost. The second class of models, the so-called "parametric models", assumes that the wave height distribution p(H) and the breaking probability conform to distributions whose shapes are *a priori* known all along the bathymetric profile. By combining these distributions with a dissipation rate per breaking wave, the total dissipation term $\overline{D}$ is obtained as a function of local wave and bathymetric parameters. As mentioned in Table 1, three such parametric models together with a model based on turbulence considerations for monochromatic waves have been implemented in TOMAWAC :

• Battjes and Janssen (1978) model (BJ78) : The authors assume that the local depth limits the wave heights in the distribution to a maximum height H_m which is a function of water depth and incident conditions (Miche criterion). So the wave height distribution follows a Rayleigh distribution clipped at $H=H_m$. All the waves having a wave height of H_m are assumed to break. The dissipation rate per unit area for a breaking wave is evaluated by using the analogy with an hydraulic jump. As the breaking wave height H_m is assumed to be in the order of water depth, the combination with the fraction of breaking waves Q_b leads, after algebraic manipulations, to the formulation for the breaking dissipation rate :

$$\overline{D} = \frac{\alpha}{4} f_p \rho g H_m^2 Q_b \qquad \text{with} \quad \alpha = 1$$

H_m is given by : $\quad H_m = \dfrac{0.88}{k} \tanh\left(\gamma \dfrac{k.d}{0.88} \right) \qquad$ with $\quad 0.5 < \gamma < 0.8$

Note that in shallow-water the above criterion reduces to : $H_m = \gamma.d$.
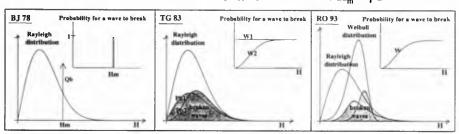

Figure 1 : Schematic diagram of parametric surf-breaking models.

• Thornton and Guza (1983) model (TG83) : Based on field observations, the authors assume a Rayleigh distribution for the wave heights even in the surf zone, but propose two different formulations for the breaking probability. The first one assumes that all waves may break with the same probability, so the repartition of breaking waves, $p_{b1}(H) = W_1(H).p(H)$ is directly proportional to the Rayleigh distribution (figure 1.b). As, in general however, the largest waves of the
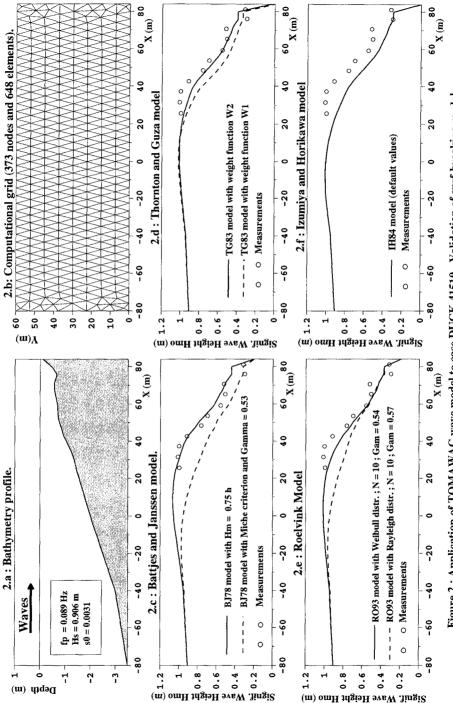
2.b: Computational grid (373 nodes and 648 elements).

2.a : Bathymetry profile.

Waves

fp = 0.089 Hz
Hs = 0.906 m
s0 = 0.0031

2.d : Thornton and Guza model

——— TG83 model with weight function W2
– – – TG83 model with weight function W1
o o o Measurements

2.f : Izumiya and Horikawa model

——— IH84 model (default values)
o o o Measurements

2.c : Battjes and Janssen model.

——— BJ78 model with Hm = 0.75 h
– – – BJ78 model with Miche criterion and Gamma = 0.53
o o o Measurements

2.e : Roelvink Model

——— RO93 model with Weibull distr. ; N = 10 ; Gam = 0.54
– – – RO93 model with Rayleigh distr. ; N = 10 ; Gam = 0.57
o o o Measurements

Figure 2 : Application of TOMAWAC wave model to case DUCK 41510 - Validation of surf-breaking models

distribution are more likely to break, another formulation W_2 (leading to $pb_2(H)$) is formulated. The average dissipation rates are obtained by combining $p_b(H)$ with a dissipation rate per breaking wave (based on bore theory) :

$$\overline{D}_1 = \frac{3\sqrt{\pi}}{16} B^3 \rho g f_p \frac{H_{rms}^7}{H_m^4 h} \quad \text{and} \quad \overline{D}_2 = \frac{3\sqrt{\pi}}{16} B^3 \rho g f_p \frac{H_{rms}^5}{H_m h} \left[1 - \left(1 + \left(\frac{H_{rms}}{H_m} \right)^2 \right)^{-5/2} \right]$$

• Roelvink (1993) model : The originality of this model lies in the use of two different functions for the distribution of wave heights, namely a Rayleigh and a Weibull distributions. The breaking probability is close to the second formulation of the TG83 model where the H_{rms} dependence is suppressed. The average dissipation terms $\overline{D}$ then read (m and A depend on local wave parameters) :

$$\overline{D}_{Weibull} = \frac{\alpha}{2} \rho g f_p \, mAH_{rms} \int_0^\infty \left(\frac{H}{H_{rms}} \right)^{2m+1} \exp\left[-A \left(\frac{H}{H_{rms}} \right)^{2m} \right] \left[1 - \exp\left(-\left(\frac{H}{\gamma h} \right)^n \right) \right] . dH$$

$$\overline{D}_{Rayleigh} = \frac{\alpha}{2} \rho g f_p H_{rms} \int_0^\infty \left(\frac{H}{H_{rms}} \right)^3 \exp\left(-\left(\frac{H}{H_{rms}} \right)^2 \right) \left[1 - \exp\left(-\left(\frac{H}{\gamma h} \right)^n \right) \right] . dH$$

• Izumiya and Horikawa (1984) model (IH84) : this model is based on the Reynolds equations and was developed for monochromatic waves propagating over a bathymetry profile. The breaking dissipation term is expressed as a function of wave energy E :

$$D = -\beta_0 \left(\frac{Cg}{C} . \frac{E}{\rho g h^2} - M_{*s}^2 \right)^{1/2} \frac{E^{3/2}}{\rho^{1/2} d^{3/2}} \left(\frac{2Cg}{C} - 1 \right)^{1/2}$$

where M_{*s}^2 is a stable wave criterion (about $0.9.10^{-2}$) and $\beta_0 = 1.8$.

(ii) Distribution of total dissipation over both frequencies and directions :

No directional dependence has been demonstrated until now, so the discussion will be restricted to the frequency dependence. Vincent et al. (1994) have analyzed laboratory data for the evolution of single-peaked spectra along a monotonic bathymetry profile. The normalised energy loss was found to be quite independent of frequency allowing the assumption that the spectral distribution of energy dissipation is directly proportional to the energy density, so that :

$$Q_{br}(f,\theta) = -\overline{D}(m_0, f_p, d) \frac{F(f,\theta)}{m_0} \quad \text{with} \quad m_0 = \int_0^\infty \int_0^{2\pi} F(f,\theta) df d\theta$$

Experiments from Beji and Battjes (1993) for waves propagating over a bar also indicate the same trend, leading to the above state-of-the-art method currently used in other wave models (Ris et al., 1994 ; Van Vledder et al., 1994).

On the other hand, Mase and Kirby (1992) observed in their laboratory experiments a frequency dependence of the breaking dissipation. They proposed to add a quadratic dependence on frequency, so that :

$$Q_{br}(f,\theta) = -(a_0 + f^2 a_1).F(f,\theta) \quad \text{with} \quad \overline{D}(m_0, f_p, d) = \int_0^\infty \int_0^{2\pi} (a_0 + f^2 a_1).F(f,\theta) df d\theta$$

As, from the observations, a linear dependence on frequency could not be excluded, both the quadratic and linear dependences have been implemented in TOMAWAC (in addition to the above classical approach neglecting any frequency dependence). The inclusion of the frequency dependence for the breaking sink term does not significantly modify the evolution of the significant wave height along the

profile. As expected however, the mean frequency is found to decrease when a quadractic dependence of frequency is activated. Indeed the higher frequencies of the spectrum are more concerned by breaking dissipation, shifting the spectral shape towards the lower frequencies. However, such a behaviour can not be validated solely, but must be analysed in conjunction with (in particular) triad interactions, which play a central role in the energy flux between the spectral components in shallow water.

(iii) Example of validation of depth-induced breaking in TOMAWAC model :

A field experiment was conducted on September 4-6, 1985, at the Field Research Facility of the U.S. Army Coastal Engineering Research Center (CERC) in Duck, North California (Ebersole and Hughes, 1987). The case presented below was recorded on September 4, 15:10 hrs (41510). The wave conditions imposed at the seaward boundary for the application of TOMAWAC are summarized on figure 2.a. The numerical simulations were carried out for the bathymetry profile shown on figure 2.a with a computational grid of approximately constant mesh (figure 2.b). The surf-breaking dissipative term was assumed to be frequency independent.

The TOMAWAC results (figures 2-c to 2-f) show that all breaking models are able to correctly reproduce the significant wave height variations along the bathymetry profile. BJ78 model was used in a first run with a value of γ determined from the Battjes and Stive (1984) formulation ($\gamma=0.53$) and with the Miche criterion for the computation of H_m (Figure 2.c). This results in an overestimation of the dissipation. In fact, Battjes and Stive formulation is not efficient for low values of steepness s_0. This test-case requires to increase γ up to 0.75, which gives quite good results. The use of the weighting function W_2 in TG83 model gives better results on this experiment than W_1 (figure 2.d), even if it does not well reproduee the wave height enhancement observed before breaking. RO93 model gives too much dissipation with the Rayleigh distribution (figure2.e), but the use of the Weibull distribution improves the results. The IH84 model is also too much dissipative (figure 2.f), but partly reproduces the wave height enhancement before breaking.

4. WAVES PROPAGATING OVER A CURRENT WHIRL

This computation has to show the capability of TOMAWAC to represent wave-current interactions on a realistic (although schematic) case of a current eddy. This case was proposed by Mathiesen (1987) as fairly representative of the whirls sometimes occurring in the nearshore zone.

4.1 Description of the test case

The spatial domain is a square of 80 km (figure 3). We consider an idealised circular whirl, centered on the origin :
- The tangential current velocity increases linearly from zero at the center of the whirl : $u(r) = u_1 \frac{r}{r_1}$ for $r \leq r_1 < r_0$
- Further away from the whirl center, the current follows a gaussian profile :

$$u(r) = u_{max} \exp\left[-\left(\frac{(r - r_0)}{b\, r_0}\right)^2\right] \text{ for } r > r_1$$

For this run, $u_{max} = 1$ m/s, $r_0 = 10$ km and $b = 0.3$, which leads to $r_1 = 9.5277$ km.
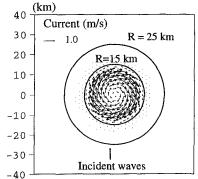

Figure 3 : Definition sketch and current field for the whirl test-case.

Mathiesen (1987) developed a semi-analytical model for this refraction problem using a ray tracing technique. This technique can be carried out upward or backward. Mathiesen used the backward ray method to determine the point (x,y,f,θ) where the energy originates to reach the point of interest. Such computations were performed for different wave frequencies and directions in order to build a complete wave spectrum. Therefore, his results can be compared with those of TOMAWAC.

The input offshore directional wave spectrum, chosen by Mathiesen (1987), is written in the form : $F(f,\theta) = S(f).D(f,\theta)$ where $S(f)$ is the frequency spectrum and $D(f,\theta)$ is the directional spreading function. The frequency spectrum is a classical JONSWAP spectrum with a peak frequency f_p equal to 0.1 Hz. $D(f,\theta)$ is based a Gaussian-shaped directional distribution :

$$D(f,\theta) = \frac{1}{\sqrt{2\pi}\,\sigma_0} \exp\left(-\frac{(\theta - \theta_m)^2}{2\,\sigma_0^2}\right)$$

θ_m is the mean incident wave direction (here $\theta_m = 0$) and σ_0 is the circular standard deviation given by the following expression :

$$\sigma_0 = \sigma_{0p}\left(\frac{f}{f_p}\right)^{-2.03} \quad \text{if } f < f_p$$

$$\sigma_0 = \sigma_{0p}\left(\frac{f}{f_p}\right)^{1.04} \quad \text{if } f \geq f_p$$

where $\sigma_{0p} = \sigma_0(f_p) = 25°$

The water depth is supposed to be constant at 200 m. The computation is achieved with Cartesian co-ordinates, without any source term (Q=0). The mesh used consists of 1876 points and 3590 elements of about 2 km on one side.

4.2 Results and discussion

Several computations were performed with TOMAWAC, using different time-steps and different directional resolutions. Only the results obtained with a time-step of 1200 s and a directional resolution of 7.5° will be presented below. The 25 discretized frequencies range from 0.04 Hz to 0.4 Hz (geometrical factor 1.1). The computed normalised significant wave height is given on figure 4. We can clearly see two zones where wave heights are enhanced separated by a zone where they are decreased. The greatest increase in wave height is obtained when waves
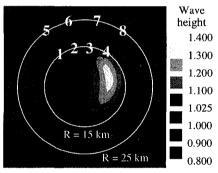
Figure 4 : Map of normalised significant wave height

propagate against the current while the greatest decrease is observed when they go the same way. The variations of significant wave height remain in the range ± 30%.
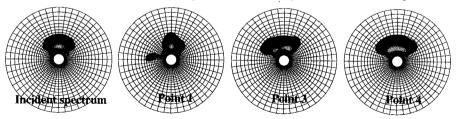
Figure 5 : Computed directional wave spectra at various locations

Figure 5 shows the wave spectra computed at various locations. We can see the presence of crossing seas, with several directional peaks in the spectrum, especially at points n°1 and 3. The directional distribution of wave energy is very inhomogeneous on this test-case. On figure 6, the directional spectra at f = 0.1 Hz are plotted for the eight points presented in figure 4. Mathiesen (1987) gives similar results with his model whose directional discretization (2.5°) was finer than ours. The TOMAWAC results compare very satisfactorily with the semi-analytical solution. The model thus appears to be able to reproduce the main features of the directional spectra, although they have a quite complex shape at several locations.
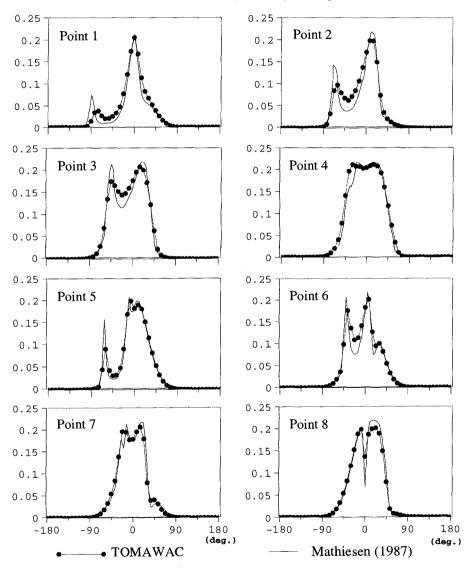

Figure 6 : Directional spectra at f = fp = 0.1 Hz - Comparison with Mathiesen (1987) model

5. SIMULATION OF THE STORM OF JANUARY 25, 1990 IN THE CHANNEL

Of all the storms to hit the Atlantic coast of France during the winter of 1989-1990, the one on January 25, 1990 was one of the most violent, with winds of force 9 to 11 (on the Beaufort scale) over French Brittany. On this particular day, the strongest gust of wind recorded at the Hague signal station was measured at 46 m/s (166 km/h). The winds blew continuously from the West, which was particularly conducive to the formation of strong waves to the West of Cotentin, and on that day, the buoys located at Ouessant registered wave heights of over 16 metres !

The period chosen for computer simulation with TOMAWAC runs from January 16 to 30, 1990, with a time-step of 5 minutes. The computational mesh consists of 6 205 nodes and 11 444 triangular elements (figure 7). The broadest meshes cover approximately 40 km on the grid boundaries, whereas the most refined ones cover less than 5 km in the English Channel. The directional wave energy spectrum has been discretized into 25 frequencies and 12 directions. The windfields (two horizontal components of the 10 m wind-speed) were provided every 6 hours from the French meteorological model results. Boundary conditions were provided by a previous simulation performed on a coarser grid covering the Northern part of the Atlantic Ocean. All source terms, including surf-breaking, were activated for this computation. The simulation was carried out without taking tidal effects into account. It required less than two hours of computing time on a Cray C98 computer for modelling an actual duration of 14 days.
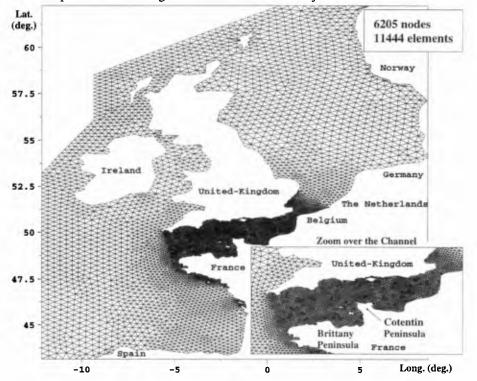

Figure 7 : Grid used for the simulation of the storm of January 25, 1990.

Figure 8 shows a chart of significant wave heights computed at the paroxysm of the storm, along with the energy spectra at the same moment at various points in the Channel. We can see that the storm's maximum intensity occurs close to the West Brittany. The further we move into the Channel, the smaller the wave heights, even though heights still manage to reach 5.5 m to the West of Cotentin (Flamanville). To validate the simulation, computational results are compared with the buoy measurements at Ouessant and Flamanville on figure 9. On both places, numerical results compare quite satisfactorily to buoy data. Furthermore, it appears from figure 8 that wave breaking significantly contributes to decrease the wave heights along the coasts of the French Brittany Peninsula.

The TOMAWAC model thus gave a good overall account of itself as far as reproducing the height of the waves was concerned, even though it slightly underestimated the January 25, 1990 peak at Ouessant. The mean periods are also fairly well reproduced, despite being generally rather overestimated by the code.
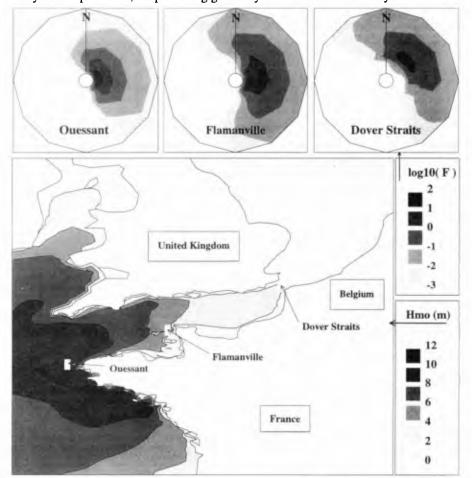

Figure 8 : Results of TOMAWAC at the peak of the storm of January 25, 1990.
(Upper plots : directional spectra ; Lower plot : map of significant wave height)
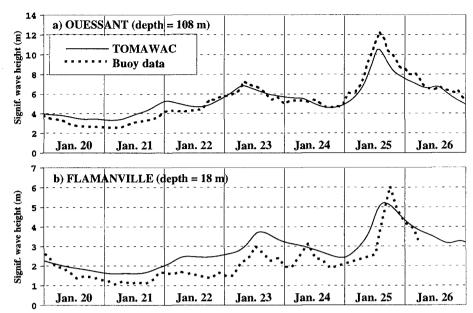
Figure 9 : Comparison of TOMAWAC results with buoy data at two locations.

6. CONCLUSIONS — FUTURE WORK

The applications presented in the previous sections show some of the capabilities of the TOMAWAC wave model, in particular for the simulation of storm waves for both offshore and nearshore areas. These cases are however only samples from the numerous test-cases performed during the validation step of the model. As a part of the TELEMAC modelling system, TOMAWAC indeed follows the Insurance Quality Procedure of EDF-LNH, with precise development rules and a complete documentation.

The inclusion of shallow-water effects such as bottom friction and depth-induced breaking has allowed to further extend the range of validity of the model towards the nearshore zone. In addition, the numerical background for spatial discretization (unstructured "finite elements" grid) and propagation scheme (piece-wise ray method) make the model very attractive for the modelling of shelf seas and shallow-water domains.

Present development efforts are dedicated to the extension of the TOMAWAC model towards the very shallow water depth, in particular by considering the non-linear interactions between triads of waves. The possibility to deal with unsteady currents and water levels is also a field of present research, in order to study the interactions between waves, storm-surges and tides.

7. ACKNOWLEDGEMENTS

8. REFERENCES

BATTJES J.A., JANSSEN P.A.E.M. (1978) : Energy loss and set-up due to breaking of random waves. *Proc. 16th Int. Conf. on Coastal Eng., Vol 1, pp 569-587*

BATTJES J.A., STIVE M.J.F. (1984) : Calibration and verification of a dissipation model for random breaking waves. *Proc. 19th Int. Conf on Coastal Eng., Vol. 1, pp 649-660*

BEJI S., BATTJES J.A. (1993) : Experimental investigation of wave propagation over a bar. *Coastal Eng., Vol. 19, pp 151-162*

BOUWS E., KOMEN G. J. (1983) : On the balance between growth and dissipation in an extreme depth-limited wind-sea in the southern North-Sea. *J. Phys. Oceanogr., Vol 13, pp 1653-1658.*

BRETHERTON F.P., GARRET C.J.R. (1968) : Wavetrains in inhomogeneous moving media. *Proc. Roy. Soc. A. 302, pp 529-554.*

CHRISTOFFERSEN J.B., JONSSON I.G. (1985) : Bed friction in a combined current and wave motion. *Ocean Eng., Vol 12, pp 387-423.*

DALLY W.R. (1992) : Random breaking waves : Field verification of a wave-by-wave algorithm for engineering applications. *Coastal Eng., Vol. 16, pp 369-397.*

EBERSOLE B.A., HUGHES S.A. (1987) : DUCK85 photopole experiment. *US Army Waterways Experiment Station, Misc. paper CEREC-87-18, Vicksburg , MS.*

ELDEBERKY Y., BATTJES J.A. (1995) : Parameterisation of triad interactions in wave energy models. *Proc. Int. Conf. Coastal Dynamics'95, pp 140-148.*

HASSELMANN S., HASSELMANN K., ALLENDER J.H., BARNETT T.P. (1985) : Computations and parameterizations of the nonlinear energy transfer in gravity-wave spectrum. Part II : Parameterizations of the nonlinear energy transfer for application in wave models. *J. Phys. Oceanogr., Vol 15, pp 1378-1391.*

IZUMIYA T., HORIKAWA K. (1984) : Wave energy equation applicable in and outside the surf zone. *Coastal Engineering in Japan, Vol. 27, pp 119-137*

JANSSEN P.A.E.M. (1991) : Quasi-linear theory of wind-wave generation applied to wave forecasting. *J. Phys. Oceanogr., Vol 21, pp 1631-1642.*

KOMEN G.J., HASSELMANN S., HASSELMANN K. (1984) : On the existence of a fully developed windsea spectrum. *J. Phys. Oceanogr., Vol 14, pp 1271-1285.*

MADSEN O.S., POON Y.K., GRABER H.C. (1988) : Spectral wave attenuation by bottom friction : theory. *Proc. 21st Int. Conf. on Coastal Eng., pp 492-504.*

MASE H., KIRBY J.T. (1992) : Hybrid frequency-domain KdV equation for random wave transformation. *Proc. 23rd Int. Conf. on Coastal Eng., pp 474-487.*

MATHIESEN M. (1987) : Wave refraction by a current whirl. *J. Geophys. Res., Vol 92, n° C4, pp 3905-3912.*

RIS R.C., HOLTHUIJSEN L.H., BOOIJ N. (1994) : A spectral wave model for waves in the near shore zone. *Proc. 24th Int. Conf. on Coastal Eng., pp 68-78.*

ROELVINK J.A. (1993) : Dissipation in random wave groups incident on a beach. *Coastal Eng., Vol. 19, pp 127-150.*

SNYDER R.L., DOBSON F.W., ELLIOT J.A., LONG R.B. (1981) : Array measurements of atmospheric pressure fluctuations above surface gravity waves. *J. Fluid. Mech., Vol 102, pp 1-59.*

THORNTON E.B., GUZA R.T. (1983) : Transformation of wave height distribution. *J. Geophys. Res., Vol. 88, N° C10, pp 5925-5938*

VAN VLEDDER G.P., DE RONDE J. G., STIVE M.J.F. (1994) : Performanee of a spectral wind-wave model in shallow water. *Proc. 24th Int. Conf. on Coastal Eng., p 761.*

VINCENT C.L., SMITH J.M., DAVIS J. (1994) : Parametrization of wave breaking in models. *Proc. Int. Symposium "Waves : Physical and numerical modelling", Vancouver (Canada), pp 753-762*

WAMDI Group (1988) : The WAM Model - A third generation ocean wave prediction model. *J. Phys. Oceanogr., Vol 18, N°12, p 1775-1810.*

WEBB D.J. (1978) : Non-linear transfer between sea waves. *Deep Sea Research, vol 25, pp 279-298.*